Relaxation of an optically created phonon void in dilute ruby

P. A. van Walree, A. F. M. Arts, and H. W. de Wijn
Faculty of Physics and Astronomy, and Debye Institute, Utrecht University, P.O. Box 80.000, 3508 TA Utrecht, The Netherlands
(Received 28 December 2000; published 3 October 2001)

A local frequency-selective depletion of phonons is created in dilute ruby at 1.8 K by optical pumping into the Zeeman-split metastable $\bar{E}(^2E)$ doublet. This phonon ''void,'' which is in dynamic balance with the spin system, is observed to recover to thermal equilibrium by an inward flow of phonons supplied from regions beyond the void, and ultimately from the helium bath. Coupled rate equations of the level populations in the void as well as the phonon density throughout the crystal account for these effects. In particular, a quartic frequency dependence of the rate for phonon transport across the crystal boundary is found, in accordance with diffuse surface scattering.

DOI: 10.1103/PhysRevB.64.174301 PACS number(s): 63.20.−e

I. INTRODUCTION

The aim of this paper is to show that a phonon ''void,'' i.e., a local depletion of phonons, can be created by optical pumping of a suitable ensemble of two-level centers, and to show how such a phonon void evolves with time as it fills with phonons moving in from the remainder of the crystal. The paper thus adds another element to the long-standing problem of the phonon bottleneck,[1] and, as the phonons ultimately have to be replenished from the helium bath, the problem of the acoustic boundary resistance.[2]

The phonon void has been realized by taking advantage of the metastable optically excited $E(^2E)$ Kramers doublet of Cr^{3+} ions in ruby ($Al_2O_3:Cr^{3+}$) at cryogenic temperatures.[3] When split in a magnetic field, the $E(^2E)$ doublet allows preferential population into its lower component ($m_S=-\frac{1}{2}$; henceforth denoted by E_-) by selective pulsed optical pumping out of the $^4A_2$ ground multiplet. As an efficient one-phonon transition connects E_- to the upper $E(^2E)$ component ($m_S=+\frac{1}{2}$; E_+), the Cr^{3+} spin system immediately starts to absorb resonant phonons so as to strive for the Boltzmann distribution $N^+/N^-=\exp(-h\nu/k_BT_0)$ associated with the crystal temperature T_0; $N^{\pm}$ denote the population densities of the levels, and $h\nu$ is the Zeeman splitting. The process of phonon absorption may conveniently be followed via the Zeeman components of the R_1 luminescence returning $\bar{E}(^2E)$ to $^4A_2$.[4]

In case the excitation density is low, ample phonons are available. The situation gains interest, however, when the initial population density residing in $E(^2E)$, N^*, is raised to such a level that the heat capacity of the spins markedly outweighs the heat capacity of the resonant lattice modes. In a simplified description, phonons are then absorbed until the spins and the phonons available near the optically pumped volume reach a common temperature substantially below T_0. In other terms, a phonon void is created. If a volume V is excited, the net number of one-phonon transitions needed to equilibrate the spins with the lattice amounts to $N_{\rm tr}=N^*p_0V/(2p_0+1)$, in which $p_0=[\exp(h\nu/k_BT_0)-1]^{-1}$ is the equilibrium phonon occupation number. In comparison, the number of thermal phonons resonant with the spins only adds up to $N_{\rm ph}=\rho\Delta\nu p_0V$, with ρ the density of phonon modes per unit frequency, and $\Delta\nu\approx55$ MHz (Ref. 3) the width of the transition. In the Debye approximation, $\rho=4\pi\nu^2/v^3$ for each direction of polarization, with v the velocity of sound. For the two transverse acoustic branches $v=6.4$ km/s.[5] Taking, as a case in point, $\nu=60$ GHz and $T_0=1.8$ K, we find $N_{\rm tr}/N_{\rm ph}\sim400$ already for excitation densities as moderate as $N^*\sim10^{22}$ m^{-3}.

After the void has been created, therefore, phonons must be furnished from the remainder of the crystal and ultimately from the helium bath surrounding the crystal in order to establish thermal equilibrium. At the frequencies considered, the thermal resistance of the crystal boundaries is still substantial, which results in a notable slowing down. In order to study the flow of phonons moving toward the void, the phonon density is followed not only in the void, but in addition in a probe volume positioned at some distance toward the crystal boundary. An accurate analysis (Sec. III) should, of course, include the spin-lattice relaxation time as well as the times characteristic for the transport of phonons through the bulk and the passage of phonons across the crystal boundary.

II. EXPERIMENTS

All measurements were performed on a cuboidal Czochralski-grown ruby crystal, having a volume of 40 mm^3 and a Cr^{3+} concentration of 500 at. ppm. The c axis is parallel to two of its faces and at an angle $\theta=65°$ with the magnetic field. To achieve optical pumping of the Cr^{3+} sustaining the phonon void, a 693-nm light pulse of 8-ns duration, resonant with the $^4A_2$, $m_S=-\frac{3}{2}\rightarrow E_-$ component of the R_1 optical transition, ran parallel to the crystal edges transverse to the field. The pulse was delivered at a rate of about 50 Hz by a dye laser, driven by a frequency-doubled Nd:YAG (yttrium aluminum garnet) laser. The laser beam was focused down to a pencil 0.3 mm in diameter. The pulse energies ranged up to 0.5 mJ, which is a compromise between strong optical pumping and avoiding damage to the crystal. The crystal was cooled to 1.8 K, at which temperature relaxation processes connecting E_+ and E_- other than by one-phonon transitions have died out.

The phonon occupation was followed in the void as well as the probe volume via optically excited Cr^{3+} ions acting as

luminescent detectors.[4] The luminescent intensity emanating from E_+ scales with N^+, which in turn is a measure for the phonon occupation number p. In the void, metastable Cr^{3+} ions are abundantly available as a result of the pulsed dye-laser excitation. To prepare the probe volume, the beam of a second frequency-doubled pulsed Nd:YAG laser was run through the sample in parallel with the primary pump beam and focused to a similar waist. Note that phonons of a particular frequency are resonant with the $E(^2E)$ doublet in small portions of the laser-excited pencils only, the remainder being out of resonance because of a finite resonance length, even in the absence of gradients in the magnetic field.[6] The horizontally oriented pencils were imaged on the vertical entrance slit of the spectrometer detecting the R_1 luminescence. The net void and probe volumes viewed, located in the bulk of the crystal, were thus confined to cylinders about 0.3 mm in diameter and 50 μm in length.

At the wavelength of the probe laser beam (532 nm), light absorption ends in the broad $^4T_2$ absorption band. After fast nonradiative multiphonon decay to $E(^2E)$, in part via the $2\bar{A}(^2E)$ doublet, the population ratio N^+/N^- is left at a nonthermal value as a result of spin memory, the partial preservation of the net spin of the $^4A_2$ ground multiplet during the optical pumping cycle.[7,8] Before the excited Cr^{3+} ions are suited to act as phonon detectors, therefore, they must be given sufficient time to achieve thermal equilibrium within $\bar{E}(^2E)$, i.e., a few milliseconds at the lowest frequencies. On the other hand, their population densities should not suffer too much from the radiative decay on the longer time scale $\tau_R \approx 4$ ms. A fair compromise is firing the probe pulse 4 ms in advance of the pulse pumping the void. This time delay also ensures removal of the nonequilibrium phonons generated in the course of the decays $^4T_2 \rightarrow {}^2E$ and $2\bar{A}(^2E) \rightarrow \bar{E}(^2E)$.

The E_+ luminescence was monitored by the use of a 0.85-m double-grating spectrometer followed by a cooled photomultiplier, photon-counting techniques, and cumulative recording. The spectrometer was tuned to the $E_+ \rightarrow {}^4A_2$, $m_S = +\frac{1}{2}$ Zeeman component, chosen for its weak reabsorption. As for the detection of N^+ in the probe volume, the effects of the phonon void were separated out by measuring the luminescent intensity in the presence (I_a) and in the absence (I_b) of a void N^*. In addition, the stray luminescence (I_c) originating from the phonon void at the probe site was determined by blocking the probe laser beam while leaving the dye laser switched on. The quantity of interest, $N^+_{\text{probe}}/N^+_{\text{probe},0}$, i.e., N^+_{probe} in relation to its thermal value, is then found from $(I_a - I_c)/I_b$. For sufficient luminescent intensity, the probe N^* needed to be of order 10% of the void N^*. It was verified that such a probe population has no marked effect on the void dynamics by a comparison of the void luminescence in the presence and absence of a probe N^*.

III. MODEL

To describe the phonon dynamics following the sudden creation of zero-temperature spin doublets and the ensuing establishment of a phonon void, we segment the crystal into shells of equal thickness, and examine the phonon densities and level populations in these shells as they evolve with time. As the phonon void is a relatively small volume located in the bulk of the crystal, these shells are centered about the void and congruent with the crystal. The free surface of the outermost shell accordingly coincides with the crystal surface. A few of the innermost shells represent the void volume as it is confined by the laser-pumped pencil and the finite resonant length of the phonons with the $E(^2E)$ doublet.[6] The remaining shells fill the rest of the crystal, one of these shells representing the probe volume by assignment of a nondisturbing spin population.

The actual calculations are greatly simplified by averaging over each individual shell. In particular, we introduce average phonon occupation numbers p_i, with $i = 1, \ldots, M$ enumerating the shells, as well as average $E(^2E)$ population densities N_i^+ and N_i^-. The approximation is not expected to detract from the essential physics, because the shells remain in compliance with the topology of void and crystal. However, it has the considerable advantage of casting the problem in the form of a limited set of coupled differential equations.

To further shape the model, we consider, for each individual shell, the rate equations for p_i, N_i^+, and N_i^-. These equations read

$$\frac{dp_i}{dt} = \frac{(p_i+1)N_i^+ - p_i N_i^-}{\rho \Delta\nu T_1} + \Gamma_{i-1\rightarrow i}(p_{i-1} - p_i) + \Gamma_{i+1\rightarrow i}(p_{i+1} - p_i), \tag{1}$$

$$\frac{dN_i^+}{dt} = \frac{p_i N_i^- - (p_i+1)N_i^+}{T_1} - \frac{N_i^+}{\tau_R}, \tag{2}$$

$$\frac{dN_i^-}{dt} = \frac{(p_i+1)N_i^+ - p_i N_i^-}{T_1} - \frac{N_i^-}{\tau_R}. \tag{3}$$

Equation (1) as shown applies to shells $i = 2, \ldots, M-1$. For the central shell ($i = 1$) the second term in Eq. (1) should be omitted, while Eq. (7) below holds for $i = M$. N_i^+ and N_i^- are nonzero only in the void and probe shells. The spin-lattice relaxation time T_1 is in the customary way defined from the point of view of the spins, which are resonant with $\rho\Delta\nu$ phonon modes. The $\bar{E}(^2E)$ state is furthermore subject to an overall slow decay back to $^4A_2$ on the time scale τ_R. As for the initial conditions, $p_i = p_0$ for all i, and $N^+ = 0$ and $N^- = N^*$ in the void shells, whereas in the probe shell N^+ and N^- start out in thermal equilibrium.

At the relevant temperatures and frequencies phonons propagate virtually ballistically, unhindered by scattering off Cr^{3+} centers[9,10] and anharmonic processes.[11] Ballistic transport through consecutive shells is incorporated into Eq. (1) through the differences $p_{i-1} - p_i$ and $p_{i+1} - p_i$ of p_i with adjoining shells. The associated rates $\Gamma_{i-1\rightarrow i}$ and $\Gamma_{i+1\rightarrow i}$ must satisfy energy conservation with due allowance for the shell volumes. Denoting the latter by V_i, we have for the passage of phonons from shell i to $i+1$ and vice versa

$$V_i \Gamma_{i+1\rightarrow i} = V_{i+1}\Gamma_{i\rightarrow i+1}. \tag{4}$$

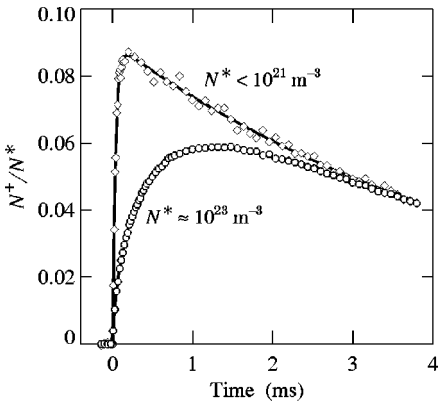

FIG. 1. The development of N^+ vs the time after selective pulsed excitation into E_- for $B=6.00$ T at $\theta=65°$, corresponding to $\nu=87$ GHz and $T_1=44$ μs. For small initial N^*, spin relaxation does not significantly disturb the phonon density. The full curve represents Eq. (8). For a substantial N^*, however, a phonon void develops, and slower spin relaxation is observed.

To comply with this condition, we define

$$\Gamma_{i\to i+1}=2V_i/(V_i+V_{i+1})\tau_1, \tag{5}$$

$$\Gamma_{i+1\to i}=2V_{i+1}/(V_i+V_{i+1})\tau_1, \tag{6}$$

where τ_1 is the time characteristic for the predominantly ballistic phonon migration from one shell to the next far away from the void. We furthermore have $V_i=(4\pi/3)[i^3-(i-1)^3](\Delta r)^3$, with Δr the average shell thickness. Note that τ_1 as defined scales with Δr, and that departures of $\Gamma_{i-1\to i}$ and $\Gamma_{i+1\to i}$ from τ_1^{-1} are strongest near the void.

The outermost shell ($i=M$) is assumed to be in contact with the second last shell and the helium bath held at temperature T_0. That is,

$$\frac{dp_M}{dt}=\Gamma_{M-1\to M}(p_{M-1}-p_M)+\frac{p_0-p_M}{\tau_2}. \tag{7}$$

A net inward flow of phonons is thus established in the event the phonon occupation within the crystal drops out of thermal equilibrium as a result of replenishment of the void.

IV. RESULTS AND DISCUSSION

We first demonstrate the creation of a phonon void by comparing, in Fig. 1, the development with time of N^+ at vanishing and substantial initial E_- populations N^*. The phonon frequency is 87 GHz. Preferring, for the moment, an approximate analytical discussion over the numerical analysis below, we consider a set of three rate equations for p, N^+, and N^- local to the void. The equations are similar to Eqs. (1)–(3), except that replenishment of p from neighboring regions is incorporated through an effective term $(p-p_0)/\tau$, with τ the typical time needed for replenishment. For vanishing N^*, we then find

$$\frac{N^+(t)}{N^*}=\frac{p_0}{2p_0+1}(1-e^{-(2p_0+1)t/T_1})e^{-t/\tau_R}, \tag{8}$$

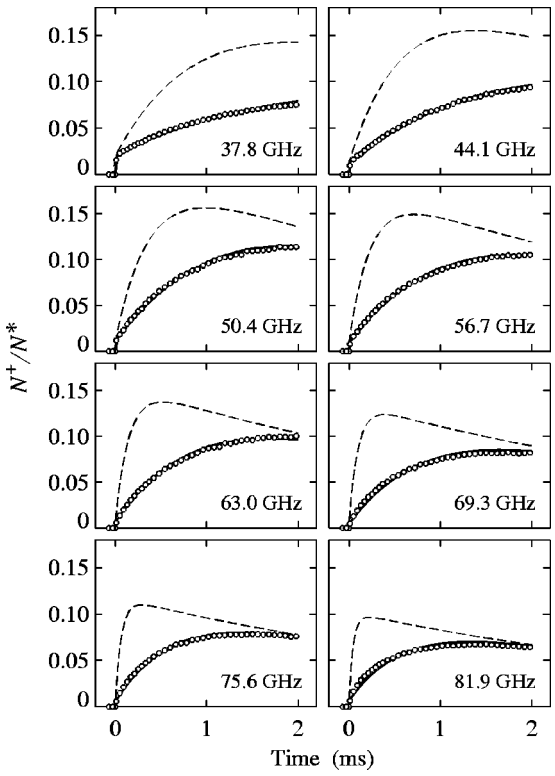

FIG. 2. The growth of N^+ in the phonon void following pulsed optical pumping of $N^*\sim 10^{23}$ m^{-3} into E_- at various phonon frequencies, as indicated. Relevant parameters are specified in Table I below. The solid curves correspond to the average of N^+/N^* weighted over the six void shells, as calculated from the model. For comparison, the development of N^+ for vanishing N^*, Eq. (8), is given as the dashed curves.

as anticipated independent of τ. The E_+ population N^+ thus tends toward its thermal equilibrium value $p_0/(2p_0+1)=0.090$ on the time scale $T_1/(2p_0+1)$ until return to $^4A_2$ takes over. For the case in point we have $T_1=44$ μs,[12,13] consistent with the experiment. For an initial $N^*\approx 10^{23}$ m^{-3}, on the other hand, so many phonons are needed to establish thermal equilibrium that the local phonon density readily becomes exhausted and the growth of N^+ is slowed down. Again resorting to the rate equations for p, N^+, and N^-, we find that $E(^2E)$ now equilibrates with the elongated time constant $T_1^*=T_1+(N^--N^+)\tau/\rho\Delta\nu$. Note that T_1^* is time dependent. Initially, $T_1^*\approx N^*\tau/\rho\Delta\nu$, but $T_1^*\to T_1$ as $E(^2E)$ equilibrates toward longer times. Indeed, $T_1^*\sim 0.3$ ms on average for a typical $\tau\sim 1$ μs.

A. Dependence on the frequency

Luminescence experiments measuring N^+ versus the time in the void as well as the probe volume were performed for a series of phonon frequencies ranging from 37.8 to 81.9 GHz, as selected via the external magnetic field. Figure 2 shows the time dependence of N^+ integrated over the phonon void, where the abscissa is cut short at 2 ms because τ_R extends over a range of values (4–6 ms) dependent on N^* and the geometry. The associated change of $N^+_{\rm probe}$ in the probe vol-

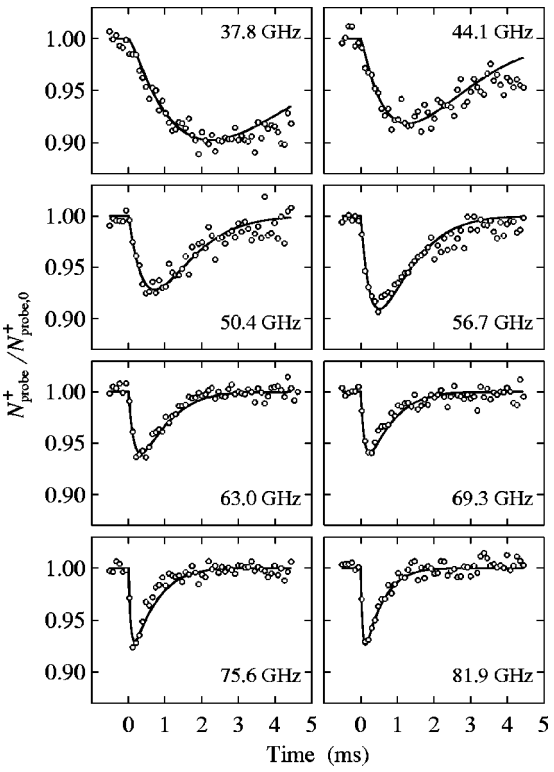

FIG. 3. The effect of the phonon void on N^+ in the probe region, normalized to its thermal value at 1.8 K. The eight frames correspond to the eight frames in Fig. 2. The establishment of a phonon void at $t=0$ leads to a transient decrease of the spin temperature beyond the void. The solid curves represent the model.

ume is shown in Fig. 3, where, as set forth in Sec. II, the effects of radiative decay are eliminated by normalizing each data point to the current thermal value $N^+_{probe,0}$. Nevertheless, the data in Fig. 3 suffer from a larger error because they were taken at a much lower N^*.

To fit the model of Sec. III to the data in Figs. 2 and 3, we numerically evaluate Eqs. (1)–(7), adjusting the initial void N^* as well as the times τ_1 and τ_2 until satisfactory fits are achieved. Here, the average ''radius'' of the outer shell is set at $R=2.1$ mm so as to match the crystal volume. A total of $M=50$ shells, each having a thickness $\Delta r=0.042$ mm, then ensure sufficiently fine spacing. The void is estimated to occupy a volume of 5×10^{-11} m^3 from the resonant length $\Lambda=0.7$ mm along the laser beam[6] in conjunction with the 0.3-mm beam diameter. In proportion, the six central shells then represent the void. With regard to Fig. 3, the development with time of N^+_{probe} at vanishing N^* was calculated for a limited number of distant shells in keeping with the distance between the probe and pump laser beams. Out of the theoretical curves for $N^+_{probe}/N^+_{probe,0}$ so obtained, the ones having $i_{probe}\sim16$ yield the best fits displayed in Fig. 3.

It is instructive at this point to consider the time scales governing the various p_i. These are $\rho\Delta\nu T_1/N_i^{\pm}$ associated with the one-phonon transitions, and τ_1 and τ_2 needed for migration. For our range of frequencies and N^*, all these times are several orders of magnitude smaller than T_1 (see Table I). The p_i, therefore, continually adjust themselves to the level populations $N^{\pm}$ as the latter evolve with time. However, τ_2 weighs in the probe p_i more heavily than in the void p_i, allowing τ_1 and τ_2 to be unraveled.

TABLE I. The parameters B, ν, T_1, and p_0 pertaining to the eight plots in Figs. 2 and 3. The quantities N^* and τ_2 result from fits of the model, as does $\tau_1=(2.1\pm0.2)\times10^{-8}$ s.

B (T)	ν [a] (GHz)	T_1 [b] (ms)	p_0	N^* (10^{23} m^{-3})	τ_2 (μs)
2.61	37.8	2.83	0.57	1.8	14
3.04	44.1	1.32	0.45	1.6	5
3.48	50.4	0.67	0.35	1.0	3
3.91	56.7	0.38	0.28	1.2	2
4.35	63.0	0.22	0.23	1.1	1
4.78	69.3	0.138	0.19	1.2	0.7
5.21	75.6	0.089	0.15	1.2	$\lesssim0.5$
5.65	81.9	0.060	0.13	1.3	$\lesssim0.3$

[a] $h\nu=(g_\parallel^2\cos^2\theta+g_\perp^2\sin^2\theta)^{1/2}\mu_B B$, with $g_\parallel=2.445$ (Ref. 3), $g_\perp=0.05$ [T. Muramoto, J. Phys. Soc. Jpn. **35**, 921 (1973)], and $\theta=65°$.

[b] Calculated from $T_1^{-1}=CB^5\sin^2\theta\cos^3\theta$ (Ref. 12), with $C=47$ T^{-5} s^{-1} (Ref. 13).

The results for N^* and τ_2 are tabulated in Table I along with other relevant parameters. The dye-laser pulse energy was kept more or less constant from one frequency to the next, which is reflected in the near constancy of the fitted N^*. It is noted that the initial N^+ observed in Fig. 2 at the lower energies stems from parasitic optical excitation over ${}^4A_2\rightarrow E_+$ as a result of the finite bandwidth of the dye laser. This initial N^+ has been taken into account in the full curves in Fig. 2, and, for a fair comparison with the relaxation in the absence of a void, in the dashed curves calculated from Eq. (8).

The third fitting parameter τ_1, associated with phonon transport from one shell to the next, was found to be $\tau_1=(2.1\pm0.2)\times10^{-8}$ s, essentially independent of the frequency in accordance with ballistic transport. Converting τ_1 to an effective velocity through $v_{eff}=\Delta r/\tau_1$, we arrive at $v_{eff}=2\pm1$ km/s for all frequencies examined, the error inclusive of the substantial uncertainties associated with averaging Δr over the shell. The reduced numerical value of v_{eff} can be largely reconciled with the velocity $v=6.4$ km/s of transverse acoustic phonons in Al_2O_3 (Ref. 5) upon noting that the average velocity of ballistic phonons leaving the crystal surface equals half the forward velocity when averaged over all possible directions. Also note that transverse phonons carry over 90% of the acoustic energy.

The most interesting observation from Table I is that τ_2 decreases steeply with increasing frequency, approximately as ν^{-4}. As in the relevant frequency regime the phonon wavelength λ is on the order of the surface roughness δ ($\lambda\approx100$ nm at $\nu=60$ GHz), phonons incident on the crystal boundaries experience strong diffuse scattering, and as a result are converted into acoustic surface, or Rayleigh, waves.[2] These waves, in turn, are scattered to phonons at either side of the boundary by defects in the adsorbed helium overlayer.

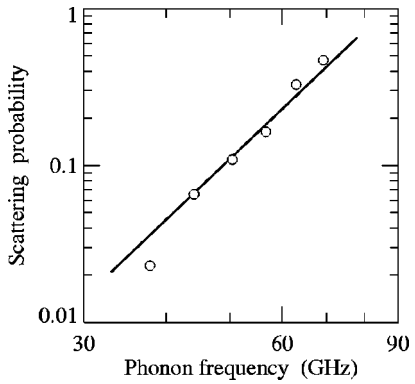

FIG. 4. The probability for diffuse phonon scattering into Rayleigh waves versus the phonon frequency. The solid line represents Eq. (9).

Theoretical calculations on diffuse surface scattering have been published by Nakayama.[14] He finds that the probability for diffuse surface scattering suffered by transverse phonons in sapphire is of the order of

$$P_{\mathrm{dif}} \sim 10^{-13} \delta^4 \nu^4, \tag{9}$$

where δ, which characterizes the size of the surface irregularities, and ν are expressed in meters and hertz, respectively. According to Eq. (9), which may be rewritten to $P_{\mathrm{dif}} \sim 10^2 (\delta/\lambda)^4$ and holds as long as $P_{\mathrm{dif}} \lesssim 1$, P_{dif} indeed becomes appreciable beyond frequencies of, say, 60 GHz in the case of polished surfaces. To convert the experimental τ_2 to P_{dif}, we compare it with the time between successive encounters of a particular phonon with the crystal surface, which we estimate at the time R/v a phonon on average needs to cross the crystal, to arrive at the data points for P_{dif} plotted double-logarithmically in Fig. 4. The straight line in Fig. 4 represents Eq. (9) with $\delta = 20$ nm, quite a reasonable value for a neatly polished ruby crystal.[15,16] At the frequencies of interest here, diffuse surface scattering in fact provides a more effective channel for energy transfer to and from the helium than does acoustic mismatch, which is regarded to be the limit of an ideal surface.[17] If $Z_{1,2}$ denote the acoustic impedances, the transmission probability against acoustic mismatch amounts to $4Z_1Z_2/(Z_1+Z_2)^2 \sim 0.003$.[2] When extrapolating the data points in Fig. 4, this value is not reached until below 20 GHz. The quantity δ self-evidently is to some extent uncertain, and so is the absolute value of P_{dif}. The agreement of the frequency dependence, however, seems sufficiently convincing to justify the conclusion that diffuse scattering dominates the boundary resistance in the frequency regime considered.

B. Dependence on N^*

To further verify the model, we have measured the phonon density in the probe volume versus the time for various initial N^* of the phonon void. In Fig. 5, the probe population N^+_{probe}, normalized to the thermal value $N^+_{\mathrm{probe},0}$, is shown versus the time for six pump pulse energies. The phonon frequency was set to 44.1 GHz, and the distance between the probe and pump laser beams was held fixed. As in Fig. 3, the quantity displayed, $N^+_{\mathrm{probe}}/N^+_{\mathrm{probe},0}$, is a measure for p in relation to its thermal value $p_0 = 0.45$, although an intricate one. Fits of the model of Sec. III to the data, displayed in Fig. 5 as the full curves, generally follow the data within the uncertainties. In particular, they reproduce the maximum drop of N^+_{probe} occurring at 1 to 2 ms, depending on the pump energy. All fits are in compliance with $v_{\mathrm{eff}} = \Delta r/\tau_1 = 2$ km/s, $\tau_2 = 4$ μs, and $i_{\mathrm{probe}} = 12$, which leaves N^* as the only parameter varying from one fit to the next. The fitted N^* is found to increase linearly with the energy of the laser pulse creating the phonon void, as it should.

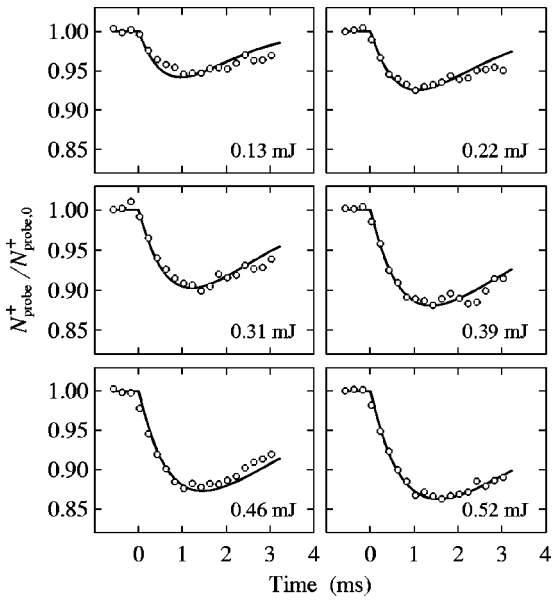

FIG. 5. The probe N^+ normalized to its thermal value versus the time for six different pump pulse energies, as indicated. The phonon frequency is 44.1 GHz. The solid curves represent the model.

C. Phonon occupation versus the distance

The effects of the void self-evidently decline with increasing distance, yet Kapitza resistance limited by diffuse surface scattering makes the phonon density fall short of the thermal value even at the crystal surface. This was verified via the probe luminescence at a phonon frequency of 63 GHz ($B = 4.4$ T; $T_1 = 0.20$ ms) and a high initial void $N^* \approx 5 \times 10^{23}$ m^{-3}. With the pulsed pump beam located close to one face of the crystal, the probe laser beam was stepwise moved toward the opposite face at 4.5-mm distance. For each position of the probe, the phonon density was determined by measuring, quite similarly to Fig. 3, the quantity $N^+_{\mathrm{probe}}/N^+_{\mathrm{probe},0}$, and extracting the minimum p reached by use of the model. The results are given in Fig. 6 in relation to p_0.

The effect of the phonon void is indeed found to decrease with increasing distance. Near the surface, however, the disturbance in p remains considerable, not dropping below $0.20p_0$. The full curve in Fig. 6 quantifies these findings. It is calculated from Eqs. (1)–(7), where a τ_2 of a few microseconds in balance with the inward phonon flow is needed to account for the drop in p at the crystal surface. Again, therefore, the model of Sec. III adequately describes the experiment. Values for τ_2 of the order of microseconds have been interpreted above in terms of diffusive scattering into Rayleigh waves.

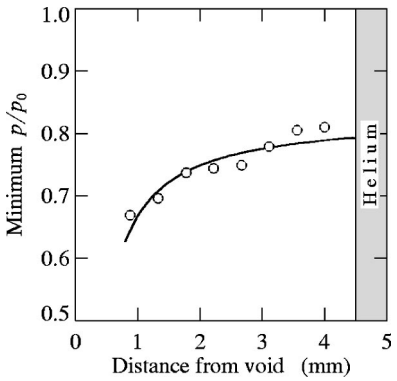

FIG. 6. The effect of the void on the phonon occupation vs the distance from the center of the void. The phonon frequency is 63 GHz. Plotted is the minimum p reached in the probe volume, normalized to $p_0=0.22$. The full curve is calculated from Eqs. (1)–(7). A sizable departure of p from p_0 is observed just below the crystal surface because of Kapitza resistance.

V. CONCLUDING REMARKS

Phonons resonant with a suitable metastable two-level system have suddenly been depleted in a confined volume by appropriate pulsed optical pumping. The ensuing recovery of this void by migration of distant phonons has subsequently been observed by the use of luminescence techniques, both in the volume itself and in a probe volume located at some distance. Position dependent rate equations adequately describe the experiments. The effective transport velocity was found to be independent of the phonon frequency, which confirms the predominantly ballistic nature of the migration at cryogenic temperatures.

The phonon void is accompanied by a spectral hole resonant with the one-phonon spin transition in an otherwise Planckian phonon distribution. In the model we have nevertheless ignored changes in the phonon frequency as a mechanism to fill the void. This is justified because at the frequencies of interest anharmonic processes have time constants running in the milliseconds at cryogenic temperatures,[11] much longer than the time needed for replenishment of the void by distant phonons. Similar considerations apply to spectral redistribution at the surface, despite the enhanced anharmonicity.[18] Indeed, to the advantage of the present model it appeared impossible to achieve a consistent fit when including anharmonic decay in lieu of exchange with the helium bath.

The spectral hole implies cooling of the lattice within the bandwidth of the phonon transition. At the higher frequencies investigated, p/p_0 in fact drops to order 10^{-2} in the core of the phonon void, corresponding to phonon temperatures of 0.6 K. If we finally take this finding together with the $p \sim 10^4$ reached in phonon avalanches, such as are launched by profuse pumping into E_+,[19–21] we see that optical pumping into the $E(^2E)$ Kramers doublet in ruby enables establishment of phonon occupation numbers spanning up to six decades. The phonon void, however, is more suited for the study of migration because of the pure incoherence of the phonons involved.

ACKNOWLEDGMENTS

The work was supported by the Netherlands Foundation ''Fundamenteel Onderzoek der Materie (FOM)'' and the ''Nederlandse Organisatie voor Wetenschappelijk Onderzoek (NWO).''

[1] Relevant papers are collected in *Spin-Lattice Relaxation in Ionic Solids*, edited by A. A. Manenkov and R. Orbach (Harper & Row, New York, 1966).
[2] E. T. Schwartz and R. O. Pohl, Rev. Mod. Phys. **61**, 605 (1989).
[3] S. Geschwind, G. E. Devlin, R. L. Cohen, and S. R. Chin, Phys. Rev. **137**, A1087 (1965).
[4] K. F. Renk, in *Nonequilibrium Phonons in Nonmetallic Crystals*, edited by W. Eisenmenger and A. A. Kaplyanskii (North-Holland, Amsterdam, 1986), p. 277.
[5] J. de Klerk, Phys. Rev. **139**, A1635 (1965); F. Rösch and O. Weiss, Z. Phys. B **25**, 101 (1976).
[6] P. A. Fokker, R. S. Meltzer, Y. P. Wang, J. I. Dijkhuis, and H. W. de Wijn, Phys. Rev. B **55**, 2934 (1997).
[7] G. F. Imbusch and S. Geschwind, Phys. Rev. Lett. **17**, 238 (1966).
[8] H. W. de Wijn and R. Adde, Solid State Commun. **27**, 1285 (1978).
[9] C. H. Anderson and E. S. Sabisky, in *Physical Acoustics VIII*, edited by W. P. Mason and R. N. Thurston (Academic Press, New York, 1971), p. 2.
[10] A. A. Kaplyanskii and S. A. Basun, in *Nonequilibrium Phonons in Nonmetallic Crystals* (Ref. 4), p. 373.
[11] Y. B. Levinson, in *Nonequilibrium Phonons in Nonmetallic Crystals* (Ref. 4), p. 91.
[12] M. Blume, R. Orbach, A. Kiel, and S. Geschwind, Phys. Rev. **139**, A314 (1965).
[13] J. I. Dijkhuis, K. Huibregtse, and H. W. de Wijn, Phys. Rev. B **20**, 1835 (1979).
[14] T. Nakayama, Phys. Rev. B **33**, 8664 (1986).
[15] P. Taborek and D. L. Goodstein, Phys. Rev. B **22**, 1550 (1980).
[16] A. G. Every, G. L. Koos, and J. P. Wolfe, Phys. Rev. B **29**, 2190 (1984).
[17] J. Weber, W. Sandman, W. Dietsche, and H. Kinder, Phys. Rev. Lett. **40**, 1469 (1978).
[18] G. Benedek and J. P. Toennies, Phys. Rev. B **46**, 13 643 (1992).
[19] J. G. M. van Miltenburg, G. J. Jongerden, J. I. Dijkhuis, and H. W. de Wijn, in *Phonon Scattering in Condensed Matter*, Vol. 51 of *Springer Series in Solid-State Sciences*, edited by W. Eisenmenger, K. Laßmann, and S. Döttinger (Springer-Verlag, Berlin, 1984), p. 130.
[20] P. A. Fokker, J. I. Dijkhuis, and H. W. de Wijn, Phys. Rev. B **55**, 2925 (1997).
[21] H. W. de Wijn, P. A. van Walree, and A. F. M. Arts, Physica B **263-264**, 30 (1999).